The Iraqi Journal For Mechanical and Material Engineering, Vol.12 , No.2 , 2012

EXPERIMETAL INVESTIGATION OF TEMPEARTURE DISTIRBUTION IN ARC FUSION WELDING

Dr. Ihsan Y. Hussain
Professor
University of Baghdad
College of Engineering
Dep. of Mechanical Engineering
Baghdad – Iraq

Dr. Salah Sabeeh Abed-Alkareem
Instructor
University of Baghdad
College of Agricultural
Dep. of Machines and Agricultural Equipment
Baghdad – Iraq

ABSTRACT
Experimental study of Heat transfer phenomena in welding process has been carried out in the present work. The experimental study was carried out on six groups (each consists of two plates) of low carbon steel material. Each plate is rectangular in shape with dimensions of (150mm x 200mm) with different thickness, (11mm) for groups (1) and (2) from A285 grade (B), ((16mm) for groups (3) and (4) from A 285 grade (C), and (19mm) for sets (5) and (6) from A285 grade (A) using single V-Butt edge design of joint welding for each group. Data Acquisition System (DAS) was manufactured and used in order to measure the transient temperature distribution of the models at the selected positions (channel (1) to channel (10)). The experimental measurements showed that the maximum temperature occurs close to the fusion region and starting to decrease a way from fusion region which is called unaffected base metal passing through the region of heat affected zone. The agreement of the results are good a comparison with present experimental work. Confirm results that were carried out experimentally. The agreement of the results is good capability and reliability the experimental steps of calculating heat transfer in Manual Metal Arc welding (MMAW).

الخلاصة

في هذا البحث، تمت دراسة عملية لانتقال الحرارة لنموذج المصدر الحراري الخطي المتحرك في عملية اللحام وكذلك ظاهرة انتقال الحرارة في عملية اللحام ألانصهاري عملياً. تضمنت الدراسة العملية اخذ القياسات العملية لنماذج عددها (6) كل نموذج يحتوي على صفيحتين من معدن الحديد منخفض الكاربون ذو الدرجات المختلفة. كل صفيحة شكلها مستطيل وذو قياسات (150 ملم × 200 ملم) لأسماك مختلفة ، (11 ملم) لنموذج رقم (1) و(2) من نوع 285 أ درجة (ب) ، (16 ملم) لنموذج رقم (3) و(4) من نوع 285 أ درجة (ج) ، (19 ملم) لنموذج رقم (5) و(6) من نوع 285 أ درجة (أ) باستعمال تصميم وصلة لحام ذو حافة تناكبية على شكل حرف V لكل نموذج . تم تصنيع منظومة اكتساب بيانات مربوطة بين الحاسوب والملحومات لتنفيذ قياسات توزيع درجات الحرارة للحالة غير المستقرة لجميع النماذج ولقنوات موزعة ومرقمة عددها (10) مختارة لتلك النماذج. القياسات العملية أظهرت بأن أعلى درجات الحرارة تحدث في القنوات القريبة من منطقة الانصهار وتبدأ بعد ذلك بالانخفاض في القنوات التي تبتعد من تلك المنطقة والتي تدعى بمنطقة المعدن الأساس الغير متأثرة بالحرارة مرورا بالمنطقة المتأثرة بالحرارة (HAZ) لتأكيد النتائج التي تم انجازها عمليا . التوافق بين النتائج جيد ويؤكد أمكانية موثوقية الخطوات العملية في حساب انتقال الحرارة بطريقة لحام القوس الكهربائي المعدني اليدوي .

KEY WORDS: Fusion Welding, Heat transfer, Numerical and Experimental Investigation

INTRODUCTION

The theory of heat flow phenomena in fusion welding process due to a moving source is of considerable importance and has broad application in the general treatment of heat flow in metals for instance in welding process. A range of important technological processes can be analyzed approximately with the aid of models that assume that a heat source of given extent moves through a medium at rest or that a stationary heat source is placed in a medium that moves through it with a constant velocity. Metal parts are commonly joined along their edges by welding. These processes rely on intense local heating by an energy source. This source moves along the seam between the two parts or the source is stationary and the parts move. A local region of melting arises. This region then cools largely by conduction into the more distant material and the parts are fused together, see Figs.(1) and (2). In all of these processes a liquid pool is formed at the seam. This solidifies as the energy source moves along the seam as heat is conducted away into the metal parts. An idealization for analysis is a moving concentrated energy source. The space above the surface is often taken as a mirror image of the processes in the material. This measure assumes that the local conduction rate heat loss in the metal parts is much greater than the surface convective and radiative losses. In these welding techniques there is a short starting process. Later the process becomes quasi-static. If the velocity of the relative motion (ν) of the heating effect remains constant then the process appears to be steady state to an observer moving at the same velocity. These metal joining processes are analyzed in attempts to improve quality control in the product; the intense local heating may cause very large thermal stresses in the immediate vicinity of the weld. Subsequent cooling and solidification leave other residual stresses in the material, **(Benjamin.1993)**. The problem was investigated in literatures with different approaches, **(Wang and Chang.1984)** found an analytical solution of the two-dimensional transient heat conduction for a finite hollow cylinder heated by a moving line source on its inner boundary and cooled convectively on the exterior. **(Adolf and Andrzej 1986)** derived a numerical method for heat transfer analysis of a solid idealized by a system of finite elements for the solution of the problem of heat flow with a moving heat source and its application in welding. **(Karlsson, et. al. 1990)** analyzed temperatures during single pass welding of a pipe using a full three-dimensional model. in their model.

The present work investigates the thermal phenomena associated with welding process, and their effects on the properties of the weldment. The research includes experimental studies. The fusion welding process, especially the electric arc welding is simulated by using the moving heat source method to calculate the transient temperature distribution in the region close to the heat affected zone and the base metal. Also the experimental work included the measurement of the transient temperature distribution of the region close to the heat-affected zone and the base metal of two plates welded by using electric arc welding process. A data acquisition system (D.A.S) technique was used.

MATHEMATICAL MODEL

Fig(3) shows a diagram of moving line source in large and very thin sheet, Consider a line source (qo) moving with constant velocity (ν) directed parallel to x-axis in a large plate with adiabatic faces. Heat losses from free surface by radiation and convection are usually negligible in welding. The properties are assumed independent of space (homogenous medium). In this case the temperature field must satisfy the energy equation, **(Salah 2005)**

$$\frac{\partial^2 T}{\partial x^2}+\frac{\partial^2 T}{\partial y^2}=\frac{1}{\alpha}\frac{\partial T}{\partial \theta}. \tag{1}$$

Because we assume medium ($\frac{\partial^2 T}{\partial z^2}=0$) , for quasi-steady state ($\frac{\partial T}{\partial \theta}=0$) and for moving heat source (ζ =x- $\nu\ \theta$)

$$\frac{\partial^2 T}{\partial \zeta^2}+\frac{\partial^2 T}{\partial y^2}=-\frac{\nu}{\alpha}\left(\frac{\partial T}{\partial \zeta}\right) \tag{2}$$

Integrating equation above we get:

$$T=e^{-(\frac{\nu}{2\alpha})\zeta} f(\zeta,y) \tag{3}$$

f is an undetermined function , The differential equation in terms of (f) and arrangment of equations gives:-

$$\frac{\partial^2 f}{\partial \zeta^2}+\frac{\partial^2 f}{\partial y^2}-\left(\frac{\nu^2}{2\alpha}\right)f=0 \tag{4}$$

For cylindrical coordinate equation becomes, see Fig. (4)

$$\frac{\partial^2 f}{\partial r^2}+\frac{1}{r}\frac{\partial f}{\partial r}+\frac{1}{r^2}\frac{\partial^2 f}{\partial \varphi^2}-\left(\frac{\nu}{2\alpha}\right)^2 f=0 \tag{5}$$

Using the properties of Bessel function obtained:

$$T=e^{-(\frac{\nu}{2\alpha})\zeta}\left[c_1 I_0\left(\frac{\nu}{2\alpha}r\right)+c_2 K_0\left(\frac{\nu}{2\alpha}r\right)\right] \tag{6}$$

$$T=T_i+\frac{q_0}{2\pi k}e^{-(\frac{\nu}{2\alpha})(x\,\nu')}k_0\left(\frac{\nu}{2\alpha}\sqrt{(x-\nu t)^2+y^2}\right) \tag{7}$$

This eq. (7) represents the transient temperature distribution field in two – dimensional case.

Initial and Boundary Conditions Representations

From, **Salah (2005)** ;

$$(1)\frac{\partial T}{\partial r}=0 \qquad at \qquad r\to\infty$$

$$(2)q_0=-KA\frac{\partial T}{\partial r} \qquad where \qquad A=2\pi r \text{ (per unit length)}$$

NUMERICAL SOLUTION

The governing equation (7) has been solved numerically to calculate the transient temperature distribution of the nodal points of the grid shown in Fig. (5). The grid has a step sizes Δx and Δy, and number of divisions NDVX and NDVY in the x- and y-direction respectively. A visual basic version (6) computer program had been built to perform the numerical calculations.

EXPERIMENTAL WORK AND PROCEDURES

The main interest of the experimental work conducted in this study was the measurements of the transient temperature distribution of the surface of the solid regions during welding process.

Experimental Facilities

The experiments were conducted in the heat transfer laboratory at the Mechanical Engineering Department, University of Baghdad.

The Groups

Six groups (each consists of two plates) of low carbon steel material has been manufactured in order to perform the experimental work. Each plate is rectangular in shape with dimensions of (150 mm×200 mm) with different thickness, (11 mm) for groups (1) and (2) from A285 grade (B) , (16 mm) for groups (3) and (4) from A285 grade (C) , and (19 mm) for groups (5) and (6) from A285 grade (A). The plates were cleaned from both surfaces and chamfered with (30^o) angle from one side, and then (10) holes of (3.4 mm) diameter were drilled at different positions and with different heights using single V-Butt edge design of joint welding for each group, see Figs. (6) and (7), and tables (1) to (6).

Data Acquisition System (DAS)

This system interfaces the computer to the welding process, in order to measure the transient temperature distribution of the models at the selected positions described previously. This system, shown in plates (I) and (II) and Fig. (8), consists of the following parts:

Amplifier

This component amplifies the electronic signal to the desired level, which the Analog to Digital Converter (ADC) can dealt with.

Multiplexer

It transports the digital signals from the amplifier to the Analog to Digital Converter in series.

Analog to Digital Converter (ADC)

Converts the analog signal to Digital Signal which can be read by the computer easily.

Decoder Circuit and Buffer

Confirmed the required control signal to the Analog to Digital Converter controller and Multiplexer, also provides a protection from any errors in control circuits and entering to output results of converter (i.e. output signal from Analog to Digital Converter) to the computer.

ISA Slot

This part is built in the mother board of computer, to extend it and to joint interface card to the mother board.

Computer and Software

A Pentium III personal computer was used to interface the DAS to the weldment test rig. A software program in Quick Basic was written in order to control the acquisition system.

Welding Machine and Electrodes

A Krakra welding machine (AC-machine) model (E-01M) fitted with an electrical power supply was used. It has a facility to weld low carbon steel (ASTM). The electrode type was (E6011) with a diameter of (2.5 mm) and (E7018) with a diameter of (3.25 mm), see Chemical Analysis % for material base metal for Gr. A, B, C and Electrode type using during welding in the tables, specification are according to ASME standards (1989). A manual Metal Arc Welding process was employed to deposit the electrode filler metal in a flat welding position.

Instrumentation

Thermocouples

A thermocouples type (K) were used to measure the temperature of the various channels mentioned previously. The calibrations of thermocouples were made at the freezing and boiling points of water and other intermediate points. To check the analogic device calibration correctly , we made comparison between measured temperatures by Thermometer and temperatures measured by thermocouple.

Thermometer

A thermometer type SIKA with range from (0˚C to 100˚C) was used to measure the room temperature.

Stop watch

Digital stop watch was used to compute the time during the welding in order to calculate the welding velocity for pass welding.

Experimental Procedure

The following procedure was followed during the experiments. Recording the room temperature by using the thermometer. Making calibration for (DAS) including all thermocouples of each channel for purpose of recording initial temperature to each channel correctly. Fixing the specimens on the table and insulated them from below thermally by using a pieces of wood. Fixing the thermocouples to the channels positions on specimens correctly. The computer program was started with welding process at the same time, and the welding time is recorded by using the stop witch, for each pass of welding. The models were left to cool down to the steady temperature. Recording the values of current and voltage used during each welding process. Storing the data in specified files for each model, see table (7) shows the experimental test parameters used in the present work.

RESULTS AND DISCUSSION

Fig. (9) shows the measured temperature history of the ten channels (positions) of plate (1) for the pass (1). It is clear that the temperature is highest at positions near the weld pool (the line heat source), and decreasing towards the heat affected zone and the base metal regions.The normal behaviour of the measured temperature history is clear in these figures. In figure (6.1) the channel 7 behaviour is abnormal and incorrect due to a thermocouple loose and movement error. It can be noted that the time required to reach the maximum temperature of the channels decreases as we go away from the line heat source. The waviness appeared in the curves of the figures during rise-up or slow-down are caused by replacing the exhausted welding wire by another one, this is called a "time delay".

The pass (1) of welding, was welding with a wire whose diameter is smaller pass (1) the level of temperatures of pass (1) is less. The time required to reach the steady state decreases with the increase of number of passes for the same plate, due to large heat lost to the surrounding air.

As the thickness of the welded plates is increased, we need more passes, and hence, high temperature levels are attained. The thinner plates are the lower levels of temperature and times are.

- Figures (10) and (12) show the results of a multipass (three passes) welding of plates (2) and (4) respectively the effect of thickness is very clear in these figures from the high levels of the temperatures and times of plate (4) compared to that of plate (2). The effect of location of the first four channels (1,2,3 and 4) on the temperature levels is higher in the high thickness plate.
- Figure (11) presents the temperature history of plate (3) for a four passes welding. The time required to reach the steady state was (2750 second).

Figure (13) shows the temperature history of plate (5) for a seven passes welding. The low level of temperature of channel (2) is incorrect due to a loose occurred in its thermocouple. The high level of temperatures due to large number of passes is clear in the figures.

Figure (14) shows the measured temperature history of plate (6) for five passes welding. A normal trend of variation is observed in the figure.

CONCLUSIONS

1) The temperature decreasing from the region close to the heat affected zone (HAZ) to unaffected base metal zone and it can be noted that the time required to reach the maximum temperature of the channels decreases as we go a way from the line heat source.
2) The time required to reach the steady state decreases with the increase of number of passes for the same plate, due to large heat lost to the surrounding air.
3) As the thickness of the welded plates is increased, we need more passes of welding, and hence, high temperature levels are attained. The thinner the plates are, the lower the level of temperature and times, and the single pass welding attained the steady state faster because less effect of temperature in the fusion region .
4) The peak point temperature of each single pass of multipass welding is reached to the same level . This means that the cooling rate between passes of multipass is very small.

Table 1 Channels Positions for Group (1)

Thickness = 11 mm

Point No.	x (mm)	y (mm)
1	40	9
2	80	9
3	120	9
4	160	9
5	40	15
6	120	15
7	40	32
8	120	32
9	40	50
10	120	50

Table 2 Channels Positions for Group (2)

Thickness = 11 mm

Point No.	x (mm)	y (mm)
1	40	13
2	80	13
3	120	13
4	160	13
5	40	19
6	120	19
7	40	45
8	120	45
9	40	71
10	120	71

Table 3 Channels Positions for Group (3)

Thickness = 16 mm

Point No.	x (mm)	y (mm)
1	40	11
2	80	11
3	120	11
4	160	11
5	40	17
6	120	17
7	40	39
8	120	39
9	40	61
10	120	61

Table 4 Channels Positions for Group (4)

Thickness = 16 mm

Point No.	x (mm)	y (mm)
1	40	8
2	80	8
3	120	8
4	160	8
5	40	14
6	120	14
7	40	28
8	120	28
9	40	44
10	120	44

Table 5 Channels Positions for Group (5)

Thickness = 19 mm

Point No.	x (mm)	y (mm)
1	40	14
2	80	14
3	120	14
4	160	14
5	40	21
6	120	21
7	40	49
8	120	49
9	40	77
10	120	77

Table 6 Channels Positions for Group (6)

Thickness = 19 mm

Point No.	x (mm)	y (mm)
1	40	11
2	80	11
3	120	11
4	160	11
5	40	17
6	120	17
7	40	39
8	120	39
9	40	61
10	120	61

		Chemical Analysis %										
Material(ASTM) Base Metal	Thickness	C	Si	Mn	Cr	Ni	Mo	P	S	Cu	V	Ti
A285 Gr. A	19mm	0.175	0.16	0.78	0.026	0.024	–	–	0.008	–	–	0.006
A285 Gr. B	11mm	0.2	0.16	0.83	0.015	0.012	–	–	0.004	–	–	0.005
A285 Gr. C	16mm	0.24	0.14	0.63	0.029	0.025	–	–	0.001	–	–	0.003

Electrode Type Using During Welding	C	Si	Mn	Cr	Ni	Mo	P	S	Cu	V	Ti
E6011	0.14	0.18	0.47	–	–	–	0.009	0.009	–	–	–
E7018	0.095	0.37	0.88	0.043	0.019	0.009	–	–	–	0.012	–

Table 7 Experimental Tests Parameters

Plate No.	TH (mm)	H (mm)	W (mm)	Pass No.	T_I (^oC)	I (A)	V (V)	u (m/s)	Electrode Φ (mm)
1	11	200	150	1	32	100	22	0.005	2.5
1	11	200	150	2	34	125	25	0.004	3.25
1	11	200	150	3	37	125	25	0.004	3.25
2	11	200	150	1	29	100	22	0.0044	2.5
2	11	200	150	2	66	125	25	0.0046	3.25
2	11	200	150	3	144	125	25	0.0037	3.25
3	16	200	150	1	33	100	22	0.0038	2.5
3	16	200	150	2	95	125	25	0.0034	3.25
3	16	200	150	3	144	125	25	0.0043	3.25
3	16	200	150	4	175	125	25	0.0031	3.25
4	16	200	150	1	37	100	22	0.0047	2.5
4	16	200	150	2	78	125	25	0.0042	3.25
4	16	200	150	3	129	125	25	0.0072	3.25
5	19	200	150	1	29	100	22	0.0043	2.5
5	19	200	150	2	106	125	25	0.0052	3.25
5	19	200	150	3	149	125	25	0.0046	3.25
5	19	200	150	4	190	125	25	0.0033	3.25
5	19	200	150	5	226	125	25	0.0042	3.25
5	19	200	150	6	227	125	25	0.0049	3.25
5	19	200	150	7	223	125	25	0.0036	3.25
6	19	200	150	1	32	100	22	0.0076	2.5
6	19	200	150	2	72	125	25	0.0046	3.25
6	19	200	150	3	121	125	25	0.0036	3.25
6	19	200	150	4	164	125	25	0.0052	3.25
6	19	200	150	5	185	125	25	0.0048	3.25

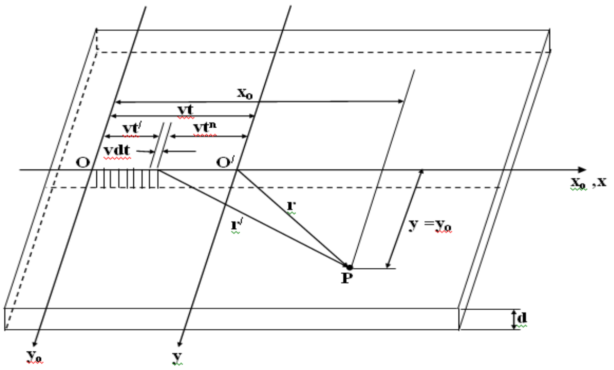

Fig. 1 . Moving Line Source in a thin Sheet, Bhadeshia (1997).

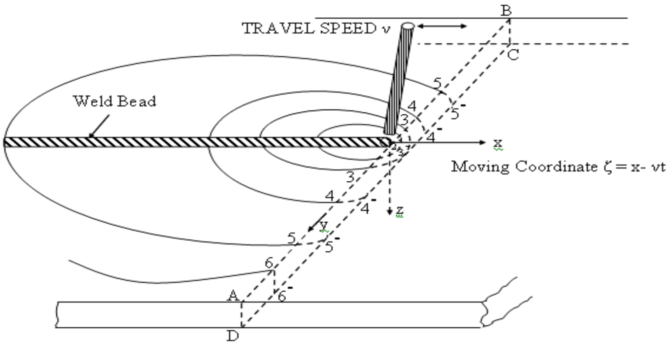

Fig. 2 . Showing the Temperature Distribution in a Plate When a Weld is Laid on the Surface, Koichi Masubuchi (1980).

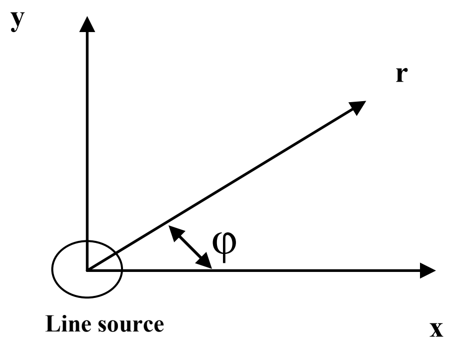

Fig. 4 . Cylindrical Coordinates

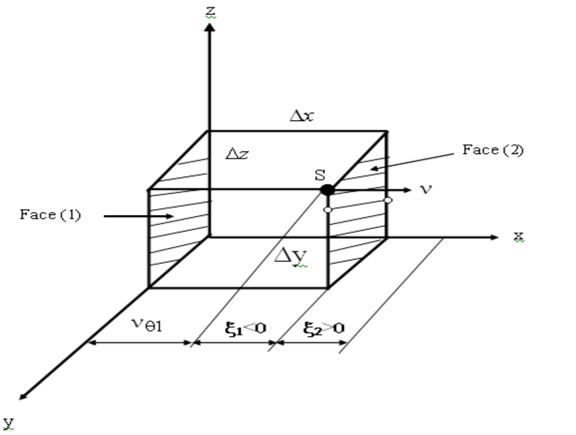

Fig. 3 . Moving Line Source in a Thin Sheet.

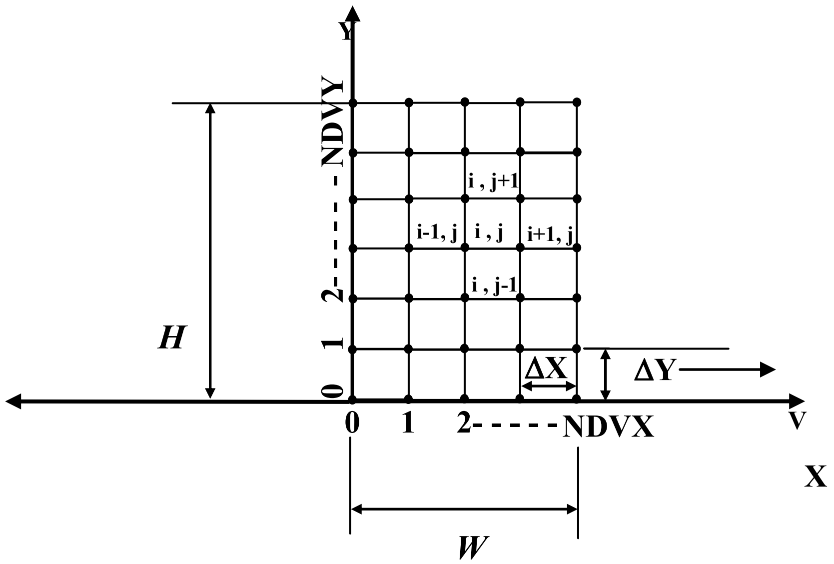

Fig. 5 . Numerical Grid Arrangement.

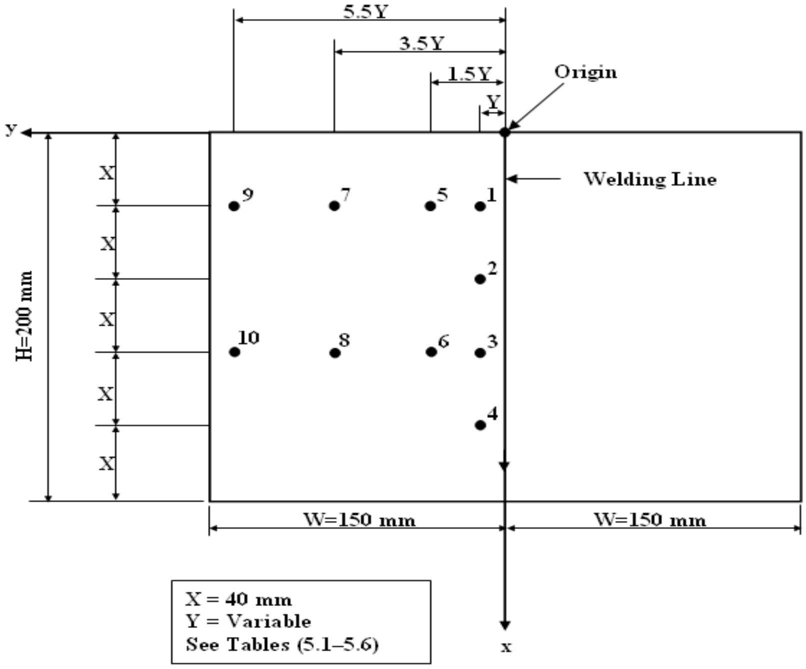

Fig. 6 . Positions of Holes of Thermocouples in the groups

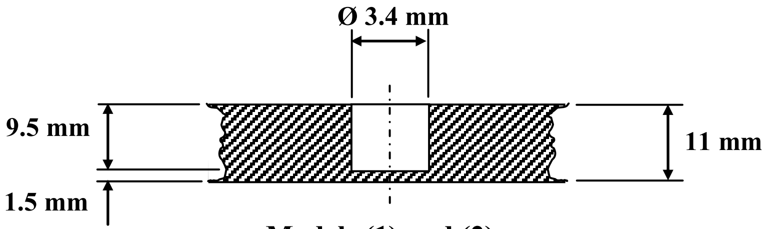

Models (1) and (2),

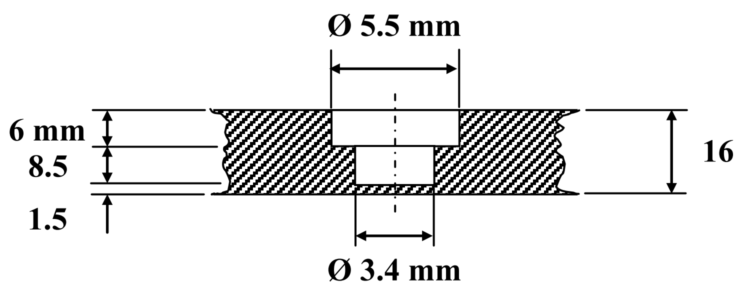

Models (3) and (4),

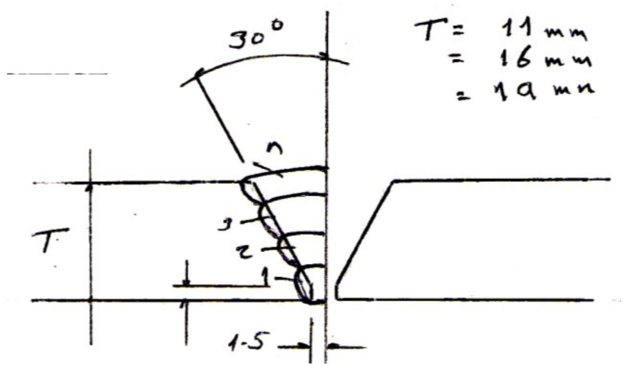

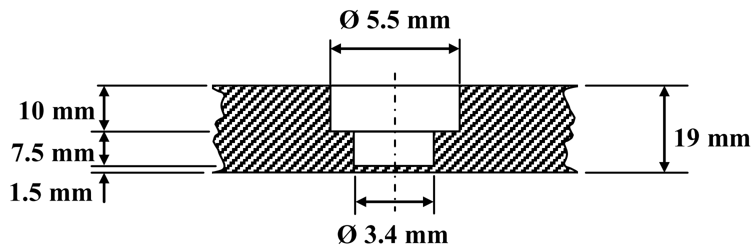

Models (5) and (6)

Fig. 7 . Details of the Holes of Thermocouples and weld design of joint

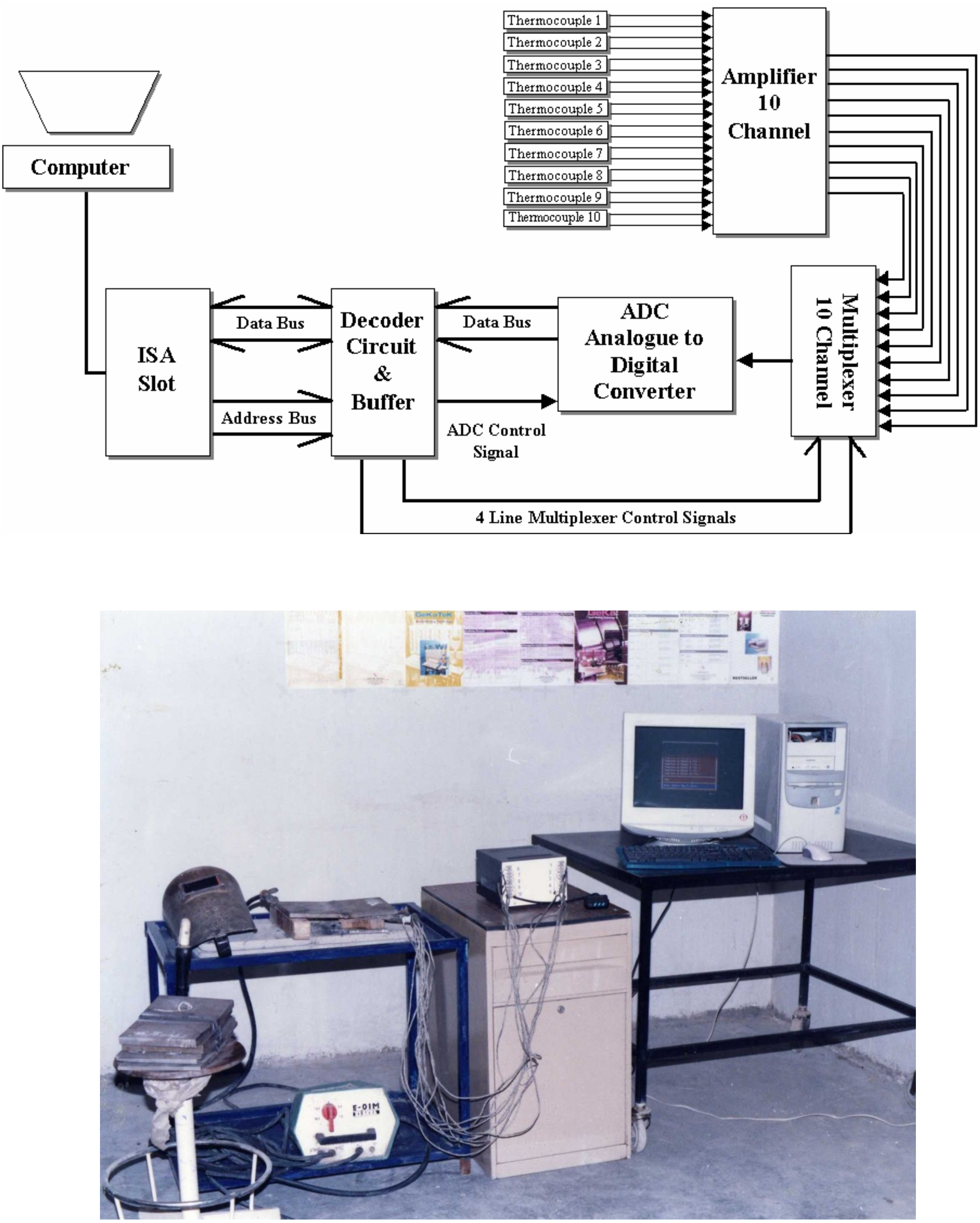

Fig. 8 . Data Acquisition System Frame and View for plates welding